Composites: Part A 46 (2013) 60–68

Contents lists available at SciVerse ScienceDirect

Composites: Part A

journal homepage: www.elsevier.com/locate/compositesa

Experimental determination and modeling of thermal conductivity tensor of carbon/epoxy composite

Maxime Villière, Damien Lecointe, Vincent Sobotka *, Nicolas Boyard, Didier Delaunay

Université de Nantes, CNRS, Laboratoire de Thermocinétique de Nantes, UMR 6607, La Chantrerie, rue Christian Pauc, BP 50609, 44306 Nantes cedex 3, France

ARTICLE INFO

Article history:
Received 28 April 2012
Received in revised form 13 September 2012
Accepted 6 October 2012
Available online 2 November 2012

Keywords:
A. Polymer-matrix composites (PMCs)
B. Thermal properties
C. Computational modeling
D. Thermal analysis

ABSTRACT

The modeling of thermal behavior of composite parts during their forming requires an accurate knowledge of their thermo-physical properties. Because of the heterogeneous nature of composites, the thermal conductivity tensor appears to be the most tricky to determine experimentally but also to model. A wide range of experimental methods can be found in the literature in order to measure either in-plane or transverse conductivity of composite parts, but very few succeed in performing it on dry preform or uncured laminates. In this study, the effective thermal conductivity tensor of carbon/epoxy laminates is investigated experimentally in the three states of a typical LCM-process: dry-reinforcement, raw and cured composite. Samples are made of twill-weave carbon fabric impregnated with epoxy resin. The transverse thermal conductivity is determined using a classical estimation algorithm, whereas a special testing apparatus is designed to estimate in-plane conductivity for different temperatures and different states of the composite. Experimental results are then compared to modified Charles & Wilson and Maxwell models. The fiber crimping of a ply is also taken into account in modeling. The comparison shows clearly that these models can be used to predict the effective thermal conductivities of woven-reinforced composites provided that the material properties are well known.

1. Introduction

Composite materials are generally distinguished by their outstanding 'strength to weight' ratio, good fatigue resistance, dimensional stability and mechanical properties. They are widely used in many applications which require high performance, such as aerospace and aeronautics industries, and more automotive industry. The knowledge of thermophysical properties is essential to control processing cycles. Indeed thermal history during processing impacts strongly the composite part quality. As a consequence, the lack of reliable data for these properties may hamper their wide utilization. Carbon-fiber reinforced polymers (CFRPs) generally show a highly anisotropic thermal behavior owing to the high thermal conductivity of carbon fibers compared to the one of the resin. Fiber orientation governs indeed the thermal conductivity tensor of composites. By considering the principal directions of the composite, this tensor is diagonal [1] and written as

$$\overline{\overline{\lambda}} = \begin{bmatrix} \lambda_x & 0 & 0 \\ 0 & \lambda_y & 0 \\ 0 & 0 & \lambda_z \end{bmatrix} \quad (1)$$

Each component can depend on temperature. In addition, the conductivity depends on the state of the composite: dry preform before injection, liquid composite after impregnation, and cured composite after crosslinking. Thus nine values of conductivity that can depend on temperature must be determined. We only present here methods used to characterize anisotropic polymer matrix composite materials and at relatively low temperature (<250 °C). Many measurement devices and methods have been developed to characterize the components of thermal conductivity tensor. Basically, they consist in thermally exciting a sample (with heater, heat flux pulse, laser, etc.) and measuring its thermal response (with thermocouples, IR camera, heat flux sensor, etc.) so as to estimate its heat transport properties. Degiovanni [2] realized a complete review of the main measurement methods. Experimental methods can be divided into two categories: thermal steady-state methods and transient ones. Among the first category, the most well-known and standardized method [3] is the guarded hot plate. The main drawback of this method lies in the fact that it only permits to estimate a unique parameter, most of the time the transverse conductivity (λ_{zz}). However it is possible to measure in-plane thermal conductivities, but only for the cured composite by machining and re-shaping the sample so as to make the heat flux cross along the desired direction. Transient methodologies can be then more efficient. In-plane components can be determined by a method called "hot wire method". It consists in radially dissipating

* Corresponding author. Tel.: +33 (0) 240683119; fax: +33 (0) 240683141.
E-mail address: vincent.sobotka@univ-nantes.fr (V. Sobotka).

1359-835X/$ - see front matter © 2012 Elsevier Ltd. All rights reserved.
http://dx.doi.org/10.1016/j.compositesa.2012.10.012

a known heat flux through a resistant wire of low section located between two homogeneous and identical materials and to measure the thermal response by micro-thermocouples located in the sample. Standard test methods based on this principle have been developed to measure thermal conductivity of some materials [4–7]. Transient Plane Source methods (TPSs) derived from works realized by Gustafsson [8,9]. This method enables to simultaneously estimate the thermal conductivity and diffusivity of homogeneous and isotropic solids based on a flat probe inserted between two identical pieces of the sample (double-sided configuration), or applied on only one side. Developments were initiated so as to estimate the in-plane $\lambda_{xx} = \lambda_{yy}$ and the transverse λ_{zz} thermal properties of orthotropic materials [10]. Thomas's method [11] derives from Gustafsson's one. It aims to simultaneously assess the components of thermal conductivity tensor and the specific heat of anisotropic composite materials without any assumption on principal directions. The parameters estimation is performed by an inverse method.

Flash method is also widely used to estimate the diffusivity of homogeneous and isotropic materials. It was extended to composite materials. This method is built upon the analysis of the back face temperature rise of a wall whose front face is submitted to an energy pulse of short time compared to the observed phenomenon. Initially proposed by Donaldson and Taylor [12] to estimate both radial and transverse diffusivity, many extensions [13–18] were developed and the whole thermal diffusivity tensor can be characterized. Measurement of the in-plane thermal gradients can be performed with thermocouples or IR-camera [19,20]. The flash method is well suited for cured composites if the matrix is not semi-transparent. Base on Ångström's method [21], periodic methods consist in heating periodically a sample. The temperature along the sample varies with the same period, but with an amplitude that decays exponentially. This principle was used to measure thermal properties of fibers contained in composite materials [22,23]. This method is efficient at small scale but has some limitation for larger scales as the ones encountered in CFRP.

The main measurement methods of effective thermal conductivities have been presented. Among all of these methods, very few manage to measure thermal conductivity on dry or liquid composite samples. An accurate determination of this property is difficult because in both cases, samples are not solid, and sealing issues have to be managed.

In this paper, we propose to determine the thermal conductivity tensor of a carbon-epoxy composite in the three states of a typical RTM process: dry-preform, uncured composite, and cured composite. A classical protocol is used for the transverse conductivity measurement and an original bench is developed for the in-plane conductivities. The principle of the second one consists in applying to a non-impregnated composite plate, initially at thermal steady-state, a temperature step in the plane of fibers and to record its evolution over its length. In-plane thermal conductivity is determined from the temperature evolution. Resin is then injected into the preform. The same protocol is followed to determine the conductivity of uncured composite. The composite is then cured. After the crosslinking a last measure is performed to determine the conductivity of the cured composite. The second step of this work consists in modeling the conductivity tensor. In the literature, plenty of models can be found to predict either longitudinal or transverse conductivities of composites for which the filler can be composed of fibers [24–30,32,33] or particles [31,32]. However, they provide different results, especially for transverse conductivity and high fiber volume fractions. Regarding longitudinal conductivity, many authors agree [26,29,31,32] that the parallel model, also called "rule of mixture" is the most suitable (Eq. (2)). Thus, the effective thermal conductivity of a unidirectional reinforced composite in a direction parallel to the fiber may be expressed by the equation

$$\lambda''_e = (1 - \Phi)\lambda_r + \Phi\lambda''_f \quad (2)$$

where Φ and λ_r denote the fiber volume fraction and the thermal conductivity of the resin, which is assumed to be isotropic, while λ''_f stands for the corresponding property of the carbon fibers, parallel to their longitudinal axis. This expression is employed in this study in the modeling of a single ply. In a second step, the different orientations of fibers in the stacking sequence are considered to obtain in-plane laminate thermal conductivities. Models predicting transverse conductivity depend mainly on the geometrical configuration of the considered reinforcement. In this study we consider the models of Charles & Wilson [24] and Maxwell [32], which are representative of UD reinforcements. A crimp angle [36] has been then introduced in these models to take into account the undulation phenomenon of the studied woven fabric.

2. Material

The materials considered in this study are representative of those used in the aeronautics industry. The reinforcement is a non-powdered 2×2 twill-weave carbon fiber fabric (G986 reference) provided by Brochier. This fabric is made of T300-type carbon fibers. These specific standard modulus carbon fibers are considered as baseline carbon fiber and are used in aerospace applications. The thermal conductivity of carbon fibers is strongly dependent on the producing process and on the precursor. Measurement of this parameter being very tricky, we computed the thermal conductivity from several papers [26,29,34,35,37] considering only T-300 type carbon fibers which are all obtained from polyacrylonitrile precursors. For this specific fiber, literature gives a scattering of ±10% on longitudinal thermal conductivity. The anisotropy of carbon fiber is taken into account considering longitudinal, λ''_f, and transverse conductivity, $\lambda^{\perp}_f$, of the fiber.

The matrix is an epoxy resin of the Hexcel Company (Ref. RTM6) whose thermal conductivities in liquid and solid states have been considered independent of temperature. DSC measurements were conducted to determine the specific heat of the reinforcement and of the resin in both states. All these properties are gathered in Table 1.

3. Transverse thermal conductivity measurement

A transient methodology is used. It allows the identification of the transverse thermal conductivity as a function of temperature of dry preform, uncured and cured composites [38]. It consists in identifying thermal conductivity from temperature measurements done at several locations through the thickness of a sample, which is placed between two heating platens, assuming 1D heat transfers. The platens are made of high conductivity beryllium-bronze alloy in order to have a homogenous surface temperature. Carbon plies are surrounded by an insulating guard which limits the lateral heat losses, and prevents the liquid resin leak under pressure. Wedges are positioned to control the thickness and hence the volume fraction of fiber in the case of measurements on dry preform. 80 μm-diameter K-type thermocouples are disposed on lateral faces and inside the sample. Their exact positions are measured afterwards, using a binocular microscope, by cutting out the sample. Temperature recordings during a typical cycle are shown in Fig. 1 for the three thermocouples in the thickness of the sample. A least-square criterion based on the difference between experimental and computed temperatures is minimized using the conjugate gradient algorithm. Numerical temperatures are computed by solving a 1D heat conduction problem, the upper and lower thermocouples acting as Dirichlet boundary conditions. The gradient of the criterion is determined by considering a set of adjoint equations [38]. Note that prior knowledge of specific heat and density of the

Table 1
Thermophysical properties of the resin and of the reinforcement (for the specific heat, T is given in °C).

Material	Density (kg m^{-3})	Specific heat (J kg^{-1} K^{-1})	Thermal conductivity (W m^{-1} K^{-1})
Carbon fiber	1770	$577.4 + 6.85165T - 0.018078T^2$	Longitudinal: 8.8 radial: 2.0
RTM6 uncured	1117	$1208.15 + 15.1969T - 0.049976T^2$	0.10
RTM6 cured	1141	$816.29 + 13.35109T - 0.036553T^2$	0.22

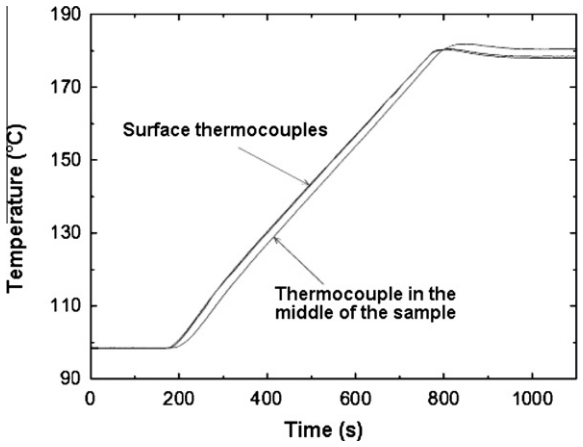

Fig. 1. Temperature rise for an uncured composite sample.

material is required for this method. Values used are those given in Table 1.The measurements were carried out for different fiber volume fractions Φ, and for balanced laminate $[0°/45°]_{n/2}$. Five fiber volume fractions have been tested in the case of the dry-preform, and two for uncured and cured laminates, these experiments being a little more delicate to conduct. Fig. 2 shows identified transverse conductivities for the dry-preforms, uncured and cured composites. One can notice a logical increase of the conductivity following the increase of Φ. Furthermore, the increase between uncured and cured composites is about 25%, to reach 0.755 W m^{-1} K^{-1} for a fiber content of 55.3%. Results show negligible influence of temperature on transverse thermal conductivities. This confirms the assumption of a constant value for the resin. Moreover, the temperature dependence of the thermal conductivity of T300 fibers was investigated by Yamane et al. [40] between 300 and 800 K, and their results showed a very low temperature dependence of the conductivity of fibers.

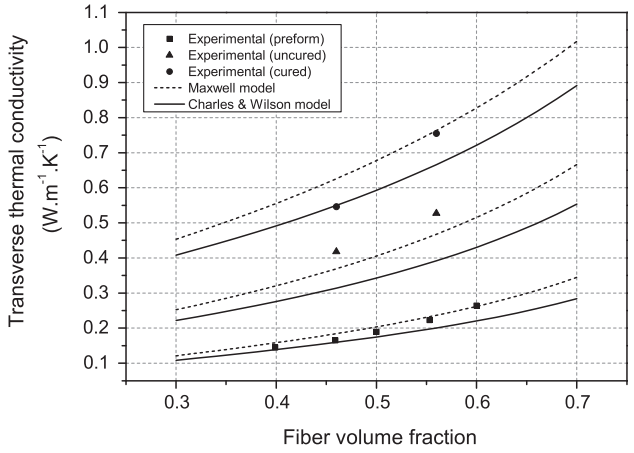

Fig. 2. Comparison between calculated and measured transverse conductivities for all states of composite and for different fiber contents.

Thus, in the following they are considered independent of temperature.

4. In-plane thermal conductivity measurement

Although the measure in the transverse direction is carried out conventionally, it is much trickier in the planar direction, heat transfer being more difficult to control in this direction. Therefore, a special apparatus has been designed for this application.

4.1. Experimental set-up

The experimental device is a small RTM mold made of Teflon® (PTFE). It is composed of two symmetrical parts and allows the molding of 60 × 70 mm^2 rectangular plates and of 10 mm thick. One half of this mold is depicted in Fig. 3 and a cross-section view in Fig. 4. In each part of this mold, a piece of copper is inserted as displayed in Fig. 4. This insert is in direct contact with the edge of the molded composite part. This mold is placed between the same heating platens described in the preceding subsection. These ones allow temperature control to the prescribed initial temperature and also to apply the required closing pressure. In addition, an aluminum sheet of 1 mm thick covers all external surfaces of the mold. This sheet acts as a thermal guard by making uniform the temperature field on the faces of the mold. In order to reduce heat losses between the lateral faces of the mold and the ambient air, the mold is surrounded by several centimeters of insulating material. The goal of this mold is to achieve a temperature step in the copper insert, so as to transfer heat in the plane of the composite. This step is obtained by suddenly circulating a coolant fluid (oil in this study) inside a channel located in this insert, at a different temperature than the one of the mold. A thermal control unit, with 0.05 K accuracy, controls the oil temperature. Since the mold is made of Teflon®, it is thermally more insulating than the carbon fiber and the composite. Therefore, during the step, heat transfer occurs mainly between the copper and the composite part. Due to the configuration of the insert (Fig. 4), the step is applied on a small surface of the composite edge allowing to obtain quickly and on a short distance a quasi uniform temperature through the thickness of the part. Thus, heat will diffuse preferentially in the plane of fibers.

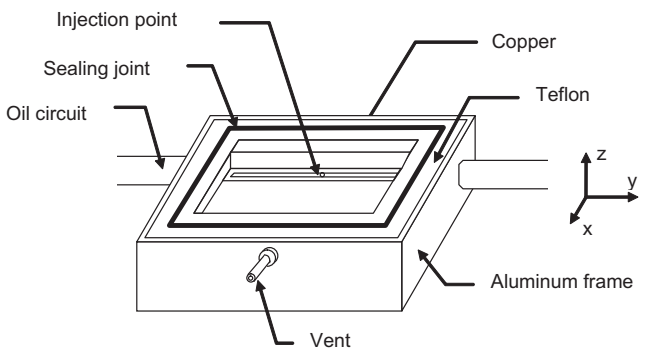

Fig. 3. Schematic of the mold.

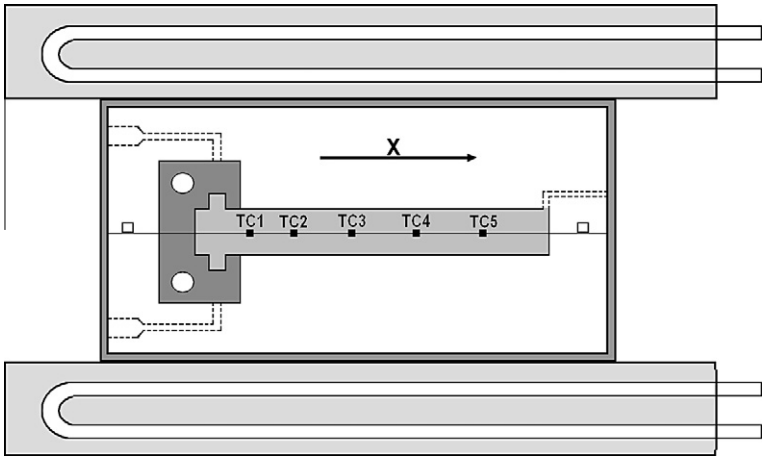

Fig. 4. Cross-section of the instrumented mold placed between the heating platens of the press.

The sample to characterize consists of two identical 5 mm thick preforms. K-type thermocouples of 80 μm are disposed in the direction of propagation of the thermal step (x-axis in Fig. 4), at half-thickness of the preform and at equal distance from lateral sides. They are placed such as their wires are along the isotherms. The temperature of the copper insert is measured by a thermocouple TC_0 fixed under it (Fig. 4). When the setting up of thermocouples is completed, the mold is placed between the heating platens of the press. A vacuum pump connected to the vent allows the injection of resin. A pressure regulator connected to the compressed air system ensures a low packing pressure after the end of the filling of the part. The temperatures are recorded using Agilent HP34970A acquisition system.

4.2. Heat transfer modeling

We assume that heat transfers occur mainly in the cross-section of the mold. A 2D conduction model is then used, for computation time reason, in the domain shown in Fig. 5. A 3D model of the mold was first used to confirm the time during which this assumption remains acceptable. A comparison between the temperature evolutions computed with 2D and 3D models shows that 3D effects cannot be neglected after 700 s. For this reason, the time used for the identification with the 2D model is limited to 500 s. Heat transfers are modeled with the following sets of equations.

In the composite part (Ω_1)

$$(\rho C_p)_{com} T^a_t = \lambda_x T^a_{xx} + \lambda_z T^a_{zz} \text{ in } \Omega_1, t > 0 \quad (3a)$$

$$-\lambda T^a_n = (T^a - T^b)/R_t \text{ on } \quad \Gamma_1, t > 0 \quad (3b)$$

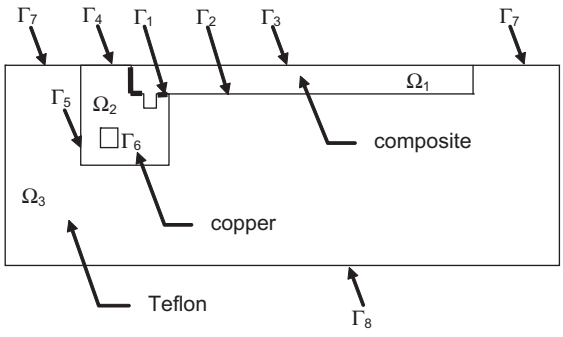

Fig. 5. 2D domain used for the heat transfer computation.

$$-\lambda T^a_n = (T^a - T^b)/R_{ptf\_com} \text{ on } \quad \Gamma_2, t > 0 \quad (3c)$$

$$-\lambda T^a_n = 0 \text{ on } \quad \Gamma_3, t > 0 \quad (3d)$$

$$T^a = T^a_{sat} \text{ in } \Omega_1, t = 0 \quad (3e)$$

In the copper insert (Ω_2)

$$(\rho C_p)_{cop} T^b_t = \lambda_{cop} \Delta T^b \text{ in } \Omega_2, t > 0 \quad (4a)$$

$$-\lambda_{cop} T^b_n = (T^b - T^a)/R_t \text{ on } \quad \Gamma_1, t > 0 \quad (4b)$$

$$-\lambda_{cop} T^b_n = 0 \text{ on } \quad \Gamma_4, t > 0 \quad (4c)$$

$$-\lambda_{cop} T^b_n = (T^b - T^c)/R_{ptf\_cop} \text{ on } \quad \Gamma_5, t > 0 \quad (4d)$$

$$T^b = TC_6 \text{ on } \quad \Gamma_6, t > 0 \quad (4e)$$

$$T^b = T^b_{stat} \text{ in } \Omega_2, t = 0 \quad (4f)$$

In the PTFE mold (Ω_3)

$$(\rho C_p)_{ptf} T^c_t = \lambda_{ptf} \Delta T^c \text{ in } \Omega_3, t > 0 \quad (5a)$$

$$-\lambda_{ptf} T^c_n = (T^c - T^a)/R_{ptf\_com} \text{ on } \quad \Gamma_2, t > 0 \quad (5b)$$

$$-\lambda_{ptf} T^c_n = (T^c - T^b)/R_{ptf\_cop} \text{ on } \quad \Gamma_5, t > 0 \quad (5c)$$

$$-\lambda_{ptf} T^c_n = 0 \text{ on } \quad \Gamma_7, t > 0 \quad (5d)$$

$$T^c = T_{platen} \text{ on } \quad \Gamma_8, t > 0 \quad (5e)$$

$$T^c = T^c_{stat} \text{ on } \quad \Gamma_8, t > 0 \quad (5f)$$

In this set of equations, T^a stands for temperature field in the composite, T^b in the copper insert, and T^c in the PTFE mold. Thermal properties of PTFE and copper used in this model are given in Table 2. Thermal inertia of the composite $(\rho C_p)_{com}$ is deduced from values in Table 1, using mixture law. Values used for the transverse

Table 2
Thermophysical properties of the mold.

	λ (W m^{-1} K^{-1})	ρ (kg m^{-3})	Cp (J kg^{-1} K^{-1})
PTFE	0.26	2200	1000
Copper	401	8933	385

thermal conductivity are those estimated in the previous subsection (Fig. 2). Temperature around the PTFE (Γ_8) is considered equal to the temperature of the platen, because of the presence of the aluminum sheet and the insulating material around the mold. Due to its high diffusivity the wall temperature of the cooling channel in the copper insert (Γ_6), is considered equal to the value recorded by the thermocouple TC_0 (Fig. 4). Two thermal contact resistances are considered between the PFTE mold and respectively the composite part R_{ptf_com} on Γ_2 and the copper insert R_{ptf_cop} on Γ_5. Sensitivity analysis shows that their values do not affect heat transfer between the three elements. They are therefore imposed. Two parameters remain unknown: the composite longitudinal thermal conductivity (λ_x) which is the goal of this bench, and the thermal contact resistance (R_t) between the composite and the copper insert on (Γ_1) which does not present any interest, but whose variations are very sensitive on heat transfer. It must be then determined as well as λ_x. Note that the fifth thermocouple was not used for the estimation, owing to a low sensitivity to these parameters. A least squares criterion J is then defined by

$$J(\lambda_x, R_t) = \sum_n \sum_{k=1}^{5} (\widetilde{T}_k^n - T_k^n)^2 \tag{6}$$

where k is the thermocouple number and n is the time step. T is the computed temperature in transient state and $\widetilde{T}$ the experimental one. The criterion being convex, the couple (λ_x, R_t) that minimizes J can easily be deduced from these variations. A double scanning on the parameters range $[\lambda_x,\ R_t] = [1;4] \times [10^{-4};10^{-1}]$ allows the determination of the absolute minimum of J.

4.3. Sensitivity analysis

The sensitivity of the temperature to key parameters is calculated at the location of the five thermocouples (TC_1–TC_5). This analysis aims to highlight the relevance of the bench design for the estimation of the unknown parameters. It also allows to make sure that the two estimated parameters are not correlated. The reduced sensitivity X_p of the variable Z to a parameter p is expressed by

$$X_p = p\frac{\partial Z}{\partial p} \tag{7}$$

The sensitivities of T to the parameters, ρCp, λ_z, λ_x and R_t have been calculated. Graphics in Fig. 6 show the sensitivities to this parameter.

The sensitivities to thermal inertia ρCp are the largest. It is therefore necessary to determine accurately these parameters. The sensitivity to the transverse conductivity λ_z is significant only for the first thermocouple, as expected, since it is located in a domain close the copper insert where 2D effects remain. On the contrary, the sensitivity to the in-plane thermal conductivity λ_x (to identify) is satisfactory for thermocouples 2–5. The thermocouple N°1 has a low sensitivity to this parameter. Nevertheless, this sensor is essential for the identification of thermal resistance R_t between the copper and the composite as shown by the curves of sensitivities to R_t (Fig. 6d).

Moreover, the sensitivity of the in-plane conductivity λ_x has been plotted (Fig. 7) as a function of the sensitivity of R_t for each thermocouple. One can notice that the slopes differ from 1, showing that the two estimated parameters are not correlated.

4.4. Measurements and results

Three fiber volume fractions (ϕ) with balanced lay-ups were tested. A fourth sample validated the measurements reproducibility. Results are summed up in Table 3. For the whole set of parts, lay-up being balanced, conductivities λ_x and λ_y are identical. A measurement cycle allows estimating for each composite part the in-plane thermal conductivities of the dry preform, the composite at raw and cured states. A complete measurement cycle can be decomposed in several stages (Fig. 8):

1. Preheating the mold at 130 °C.
2. Measurement on the dry preform: a temperature step is created by opening the valve that controls oil flow. Oil temperature is set to 80 °C.
3. Preparing the injection part: homogenization of the mold temperature, preheating and degassing the resin, vacuum the preform.
4. Injection of the resin in the mold. Application of a 0.5 bar holding pressure.
5. Homogenization of the mold temperature. This phase should be short enough (less than 30 min) to avoid the beginning of the crosslinking of the resin.
6. Measurement on the liquid composite.
7. Curing of the composite part: temperature of the heating platens is set at 180 °C.
8. Measurement on the cured composite. Data recorded during this phase are not shown in Fig. 8 because the whole cycle lasts more than a day. The measurement on the cured composite is realized in the same way as for the raw state after thermal steady-state is reached.

Identification procedure leads to a good agreement between experimental and numerical temperatures. The standard deviation between temperatures remains low (between 0.2 °C and 0.7 °C) in comparison with the amplitude of the temperature step (50 °C). The residuals for the cured part N°2 are shown in Fig. 9. Table 4 sums up the evolution λ_x versus the fiber volume content. Except for the value of the sample N°2 (ϕ = 53.3%) in the cured state, we observe consistent results. As expected, in-plane thermal conductivities can be 10 times higher than transverse conductivities. The values increase from 3.0 W m^{-1} K^{-1} for the dry preform (ϕ = 60%) to 3.7 W m^{-1} K^{-1} for the cured part. During the curing, an increase of only 10% occurs whereas it is of 25% for the transverse direction and more than 100% for the pure resin. This evolution is indeed expectable since thermal conductivity in planar direction is governed by carbon fiber and not by resin. The values of the identified thermal contact resistances (TCR) are plotted in Fig. 10. They decrease then strongly after the injection of the resin at the raw state, revealing a significant improvement of the contact between the sample and the copper insert. Finally, we observe a logical increase of this value after crosslinking, the contact being affected by the chemical shrinkage. Thermal contact resistance values for the raw composite are close to 5e−3 m^2 K/W. This large value can derive from several factors. The resistance estimated on Γ_1 actually includes two edges (Fig. 5). The cutting of the reinforcement being imperfect, all fibers do not touch the lateral outer edge of the copper insert. As a consequence, the area near the copper insert contains more resin, acting as an additional thermal resistance. Moreover during the experiments described in this paper, no holding pressure was imposed after the end of the filling. The molding cavity remained at atmospheric pressure during the measurement.

5. Modeling of thermal conductivities

The two-step method used in this part was developed by Kulkarni and Brady [24]. The first step consists in determining the transverse and longitudinal thermal conductivities of a single unidirectional lamina in which the fibers are parallel, as shown in Fig. 11. In the second step, the different orientations of fibers in the stacking sequence are considered to obtain the laminate

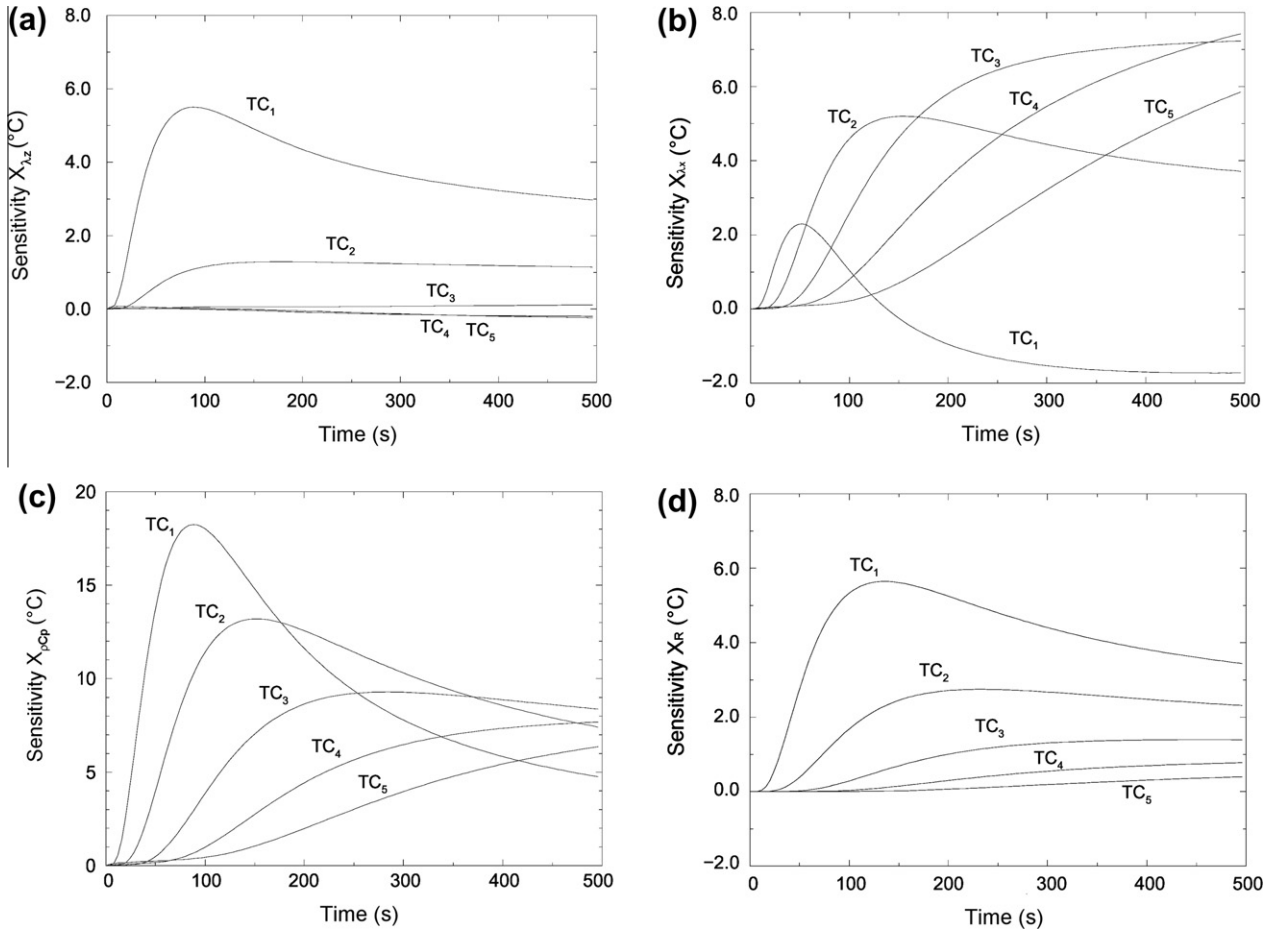

Fig. 6. Temperature sensitivities to parameters: λ_z (a), λ_x (b), ρCp (c) and R_t (d).

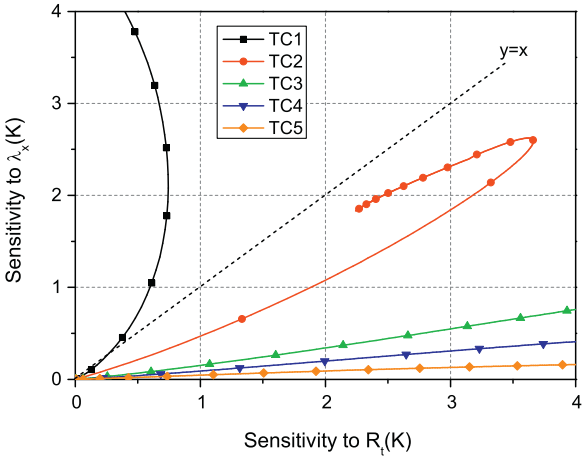

Fig. 7. Parameters correlation. (For interpretation of the references to colour in this figure legend, the reader is referred to the web version of this article.)

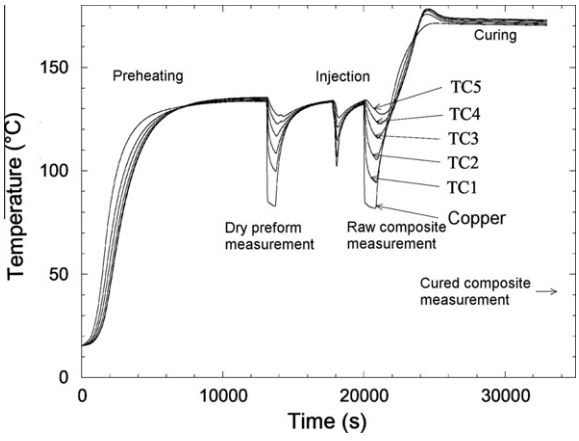

Fig. 8. Measurements during a molding cycle.

Table 3
Configuration of the samples.

Part N°	ϕ (vol%)	Plies number (n)	Lay-up
1	40.0	24	$[0°/45°]_{12}$
2	53.3	32	$[0°/45°]_{16}$
3	60.0	36	$[0°/45°]_{18}$

thermal conductivity tensor. We provide here a modified model that adapts to the case of woven reinforcements. The thermal conductivity parallel to the fiber direction, λ_1 (Fig. 11) is easily obtained by the parallel model, or rule of mixtures, by Eq. (1). In the transverse direction of the lamina (λ_2 or λ_3), the conductivity may be calculated by the Charles & Wilson's model [24].

$$\lambda_{2CW} = \lambda_r \left[\frac{\lambda_f^{\perp}(1+\Phi) + \lambda_r(1-\Phi)}{\lambda_f^{\perp}(1-\Phi) + \lambda_r(1+\Phi)} \right] \tag{8}$$

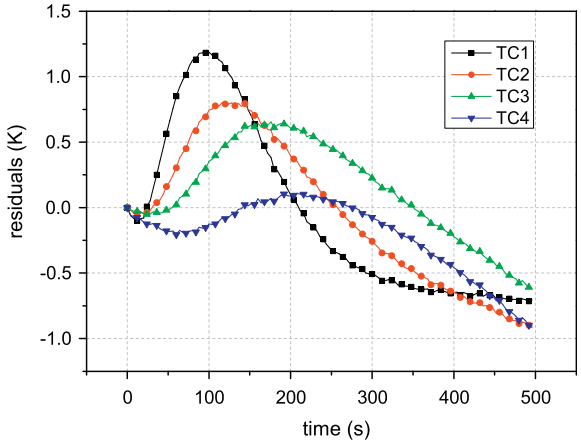

Fig. 9. Residuals for the cured part N°2. (For interpretation of the references to colour in this figure legend, the reader is referred to the web version of this article.)

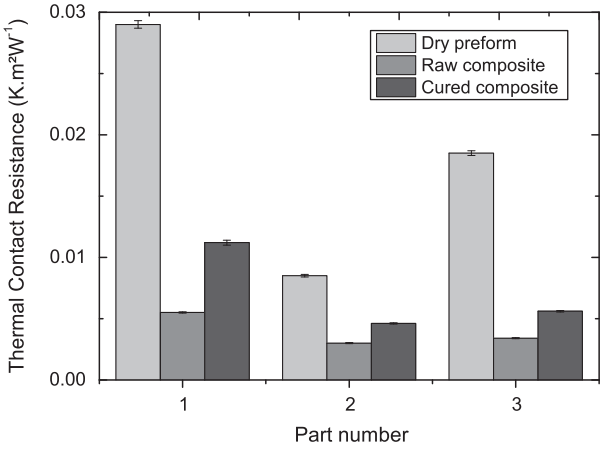

Fig. 10. Identified thermal contact resistances.

Based on a potential analogy, Maxwell [32] obtained a quite similar relationship for the conductivity of randomly distributed and non-interacting discs in a homogenous matrix.

$$\lambda_{2M} = \lambda_r \left[\frac{\lambda_f^{\perp} + 2\lambda_r + 2\Phi(\lambda_f^{\perp} - \lambda_r)}{\lambda_f^{\perp} + 2\lambda_r - \Phi(\lambda_f^{\perp} - \lambda_r)} \right] \tag{9}$$

In both models, the interactions between fibers are ignored: it is therefore assumed that there is no contact between them. Although it fails to predict the correct behavior when $\Phi \to \Phi_{max}$, they are quite simple models that give satisfactory results for unidirectional laminae.

In order to calculate in-plane thermal conductivities of the twill-wave carbon (G986) reinforcement, this latter can be broken down into a sequence of unidirectional laminae (Fig. 12). Thus, a twill-weave fabric made up of tows at $\theta = 0°$ and $\theta = 90°$ will be split into two unidirectional laminae having as much as fibers in both directions. We assume that all laminae have identical thickness and fiber fraction. Only the fiber orientation in each ply (i) varies. Global conductivity tensor (λ_{xi}, λ_{yi}, λ_{zi}) of one ply can be obtained through conductivities of an UD-lamina (λ_1 and λ_2 in Fig. 11) by

$$\lambda_{x,i} = \lambda_1 |\cos\theta_i| + \lambda_2 |\sin\theta_i| \tag{10}$$

$$\lambda_{y,i} = \lambda_1 |\sin\theta_i| + \lambda_2 |\cos\theta_i| \tag{11}$$

$$\lambda_{z,i} = \lambda_2 \tag{12}$$

where θ_i represents the fiber orientation angle with respect to the global x-axis for a ply i. These components for a single ply are used further to infer global thermal conductivity tensor components of the fabric composite. These are obtained by stacking N plies of the

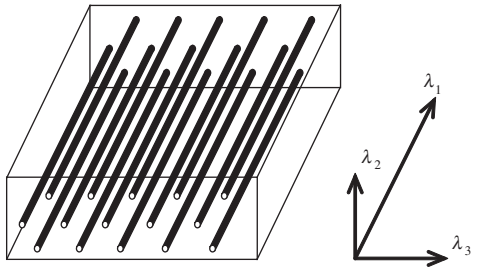

Fig. 11. Principal thermal conductivities of an individual lamina.

reinforcement and applying for the in-plane thermal conductivities a model of parallel thermal resistances

$$\lambda_d = \frac{1}{N} \left(\sum_{i=1}^{N} \lambda_{d,i} \right)_{d=x,y} \tag{13}$$

In our case, these plies are subsequently laid up under a specified stacking sequence $[0°/45°]_{16}$ so as to obtain balanced laminates, for which the thermal conductivities in x and y directions are equivalent.

And for the transverse conductivity a model of serial thermal resistances

$$\lambda_z = \frac{1}{N} \left(\sum_{i=1}^{N} \frac{1}{\lambda_{z,i}} \right)^{-1} \tag{14}$$

Considering that all laminae are identical, it comes: $\lambda_z = \lambda_2$. Fiber waviness is inherent in many reinforcing fabrics, unlike unidirectional composites, for which all fibers are nearly perpendicular

Table 4
Comparison between calculated and measured in-plane conductivities for all states of composite.

State	Part	Experimental conductivity ($W\,m^{-1}\,K^{-1}$)	Predicted conductivity (Maxwell) ($W\,m^{-1}\,K^{-1}$)	Predicted conductivity (Charles & Wilson) ($W\,m^{-1}\,K^{-1}$)	Deviation (Maxwell)	Deviation (Charles & Wilson)
Dry-preform	1	2.15	2.13	2.13	0.9%	0.9%
	2	2.70	2.81	2.81	4.1%	4.1%
	3	3.03	3.19	3.19	5.3%	5.3%
Uncured	1	2.33	2.32	2.29	0.4%	1.7%
	2	2.87	3.07	3.03	7.0%	5.6%
	3	3.40	3.47	3.41	2.1%	0.3%
Cured	1	2.62	2.50	2.46	4.6%	6.1%
	2	(2.91)	3.28	3.23	12.7%	11.0%
	3	3.73	3.68	3.62	1.3%	2.9%

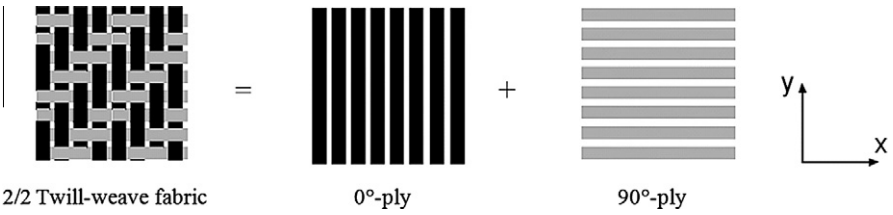

Fig. 12. Decomposition of one ply in two unidirectional laminae.

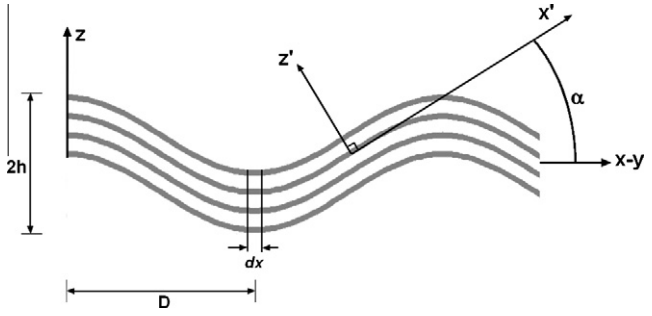

Fig. 13. Crimp angle between a yarn and x–y plane.

to the z-axis. In fact, fiber crimping can be observed in the case of woven reinforcements. In such situations, each fiber bends over or under another and its axis departs from a straight line and follows a simple or complex wavy path. A model that takes account of this effect is then considered. It brings a correction to the previous estimated conductivities (Eqs. (10)–(12)). Sottos in [39] computes thermoelastic properties of fabrics by introducing a crimp factor as shown in Fig. 13. The fiber bundle undulates in the x–z plane following a cosine curve of amplitude h and wavelength 2D described by

$$z(x) = h\cos\left(\frac{\pi}{D}x\right) \tag{15}$$

If the fibers are assumed straight but oriented at an angle α over a small section dx of the yarn, the angle of rotation is given by the slope of the curve

$$\alpha(x) = \arctan\left(\frac{dz}{dx}\right) \tag{16}$$

A mean crimp angle is defined over a half period by

$$\tilde{\alpha} = \arctan\left(\frac{2h}{D}\right) \tag{17}$$

By analogy with mechanics, and considering that all laminates are identical, except their planar orientations, the transverse thermal conductivity is given by

$$\lambda_z = \lambda_1|\sin\tilde{\alpha}| + \lambda_2|\cos\tilde{\alpha}| \tag{18}$$

Even for the case of small angles, conductivity λ_1 (Eq. (1)) being larger than λ_2 (Eqs. (8) and (9)), the resulting value for λ_z is increased. On the contrary, in the plane, a low value of the angle does not impact conductivities. Indeed, carbon fibers conduct heat much better than the resin, then they govern accordingly planar conductivity. By micrographic observations, we measured the average crimp angle $\tilde{\alpha}$ in a cured laminate using Eq. (16). We find $2h$ = 11 mm and D = 6.2 mm. Thus, we obtain $\tilde{\alpha} = 1^\circ$.

Results are gathered in Fig. 2 and Table 4 respectively for the transverse and in-plane conductivities. Data used in the models are those of Table 1. Experimental and computed values are in very acceptable agreement except for the in-plane value of the cured composite part N°2 (Table 4), which may be imputed to a measurement error. Concerning the transverse conductivity dry-preform and cured laminate results are fitted between the two analytical models regardless of the fiber content. Moreover, it seems that the Maxwell model is more suitable for high fiber volume fractions and that Charles & Wilson is more effective for lower fiber contents. Nevertheless, this latter underestimates uncured transverse conductivity by a maximum of 20.9% and 33.2% respectively for fiber volume fractions of 46% and 55.3%. Maxwell model is slightly better, the deviation being lower than 13%, which represents about only 0.06 W m^{-1} K^{-1}. This large scattering indeed highlights the importance to determine accurately the liquid resin conductivity, to which both models are extremely sensitive. However one can notice both models are not sensitive to the radial value of carbon fiber $\lambda_f^{\perp}$.

In-plane conductivities are also modeled using Maxwell and Charles & Wilson models. There is no marked difference between the trends of both models. A mean deviation of 3% is observed between experimental and calculated conductivities for the whole set of values (except for cured part N°2). For the dry preform estimation, conductivities determined using both models are identical since conductivity in transverse direction λ_2 is 0, preform being under vacuum.

Moreover, both models are very sensitive to fiber volume fraction and to the longitudinal conductivity of fiber. This last parameter should be investigated since values found in literature [26,29,34,35,37] are relatively scattered.

6. Conclusion

By combining two methods of measurement, the determination of the transverse and in-plane thermal conductivities in all states of a typical LCM process was achieved. While transverse thermal conductivities were identified by a classical transient methodology coupled to an inverse method, in-plane thermal conductivities were determined on an original home-made bench. In comparison with other characterization devices, this one makes it possible to estimate the conductivities during the different stages of the molding: from the dry preform, to the raw composite and finally to the cured composite. The experimental bench and the identification algorithm developed have provided results which give good agreement between computed and experimental temperatures. In-plane heat transfer is described with a satisfactory accuracy. The deviations between the measured and the computed temperatures are lower than 1.2 K for temperature amplitude of more than 50 K. Basic models have been used to predict the thermal conductivity tensor. They have been simply improved by introducing the crimp angle that takes into account the waviness of a real fabric. In spite of their simplicity, they provide satisfactory predictions of the thermal conductivity tensor of the fabric.

Our results confirm that the uncertainties on the thermal conductivities of the constituents and of the resin volume fraction are of paramount importance on the reliability of the predictions of the models. A more sophisticated model is not relevant until

an accurate measurement of the thermal conductivity of the raw resin and of the fibers is not performed. Contrary to the resin, the measurement for the fiber is much more difficult since efficient methods are not usual yet.

An improvement of the method will consist in identifying simultaneously the in-plane and transverse conductivities and specific heat of the material using a more effective identification method. A new apparatus is being designed to achieve this issue.

References

[1] Ozisik MN. Heat conduction. John Wiley & Sons Inc.; 1993.
[2] Degiovanni A. Conductivité et diffusivité thermique des solides. Techniques de l'ingénieur 1994;R2:850.
[3] Norme ISO 8302:1991. Isolation thermique – détermination de la résistance thermique et des propriétés connexes en régime stationnaire – méthode de la plaque chaude gardée, 1991.
[4] Norme ISO 8894–1. Matériaux réfractaires – détermination de la conductivité thermique, 1987.
[5] Lobo H. Thermal conductivity and diffusivity. In: Dekker M, editor. Handbook of plastics analysis, 2003.
[6] Standard ISO 22007–1. Plastics – determination of thermal conductivity and diffusivity, 2006.
[7] Jarny Y, Guillemet P. Estimation simultanée de la conductivité thermique et de la chaleur spécifique de matériaux orthotropes. In: Proceedings of SFT conference; 2001, p. 609–14.
[8] Gustafsson SE. Transient plane source techniques for thermal conductivity and thermal diffusivity measurements of solid materials. Rev Sci Instrum 1991;62(3):797.
[9] Gustavsson M, Karawacki E, Gustafsson SE. Thermal conductivity, thermal diffusitvity and specific heat of thin samples from transient measurement with Hot Disk sensors. Rev Sci Instrum 1994;65(12):3856–9.
[10] Gobbé C, Iserna C, Ladevie B. Hot strip method: application to thermal characterisation of orthotropic media. Int J Therm Sci 2004;43(10):951–8.
[11] Thomas M, Boyard N, Lefèvre N, Jarny Y, Delaunay D. An experimental device for the simultaneous estimation of the thermal conductivity 3-D tensor and the specific heat of orthotropic composite materials. Int J Heat Mass Trans 2010;53(23–24):5487–98.
[12] Donaldson AB, Taylor RRE. Thermal diffusivity measurement by a radial heat flow method. J Appl Phys 1975;46:4584–9.
[13] Degiovanni A, Bastale JC, Maillet D. Mesure de la diffusivité longitudinale de matériaux anisotropes. Rev Gén Therm 1996;35(410):141–7.
[14] Degiovanni A, Laurent M. Une nouvelle méthode d'identification de la diffusivité thermique par la méthode flash. Rev Phys Appl 1986;21(3):229–37.
[15] Demange D, Beauchike P, Bejet M, Casulleras R. Mesure simultanée de la diffusivité thermique selon les deux directions principales d'un matériau. Rev Gén Therm 1997;36(10):755–70.
[16] Lachi M, Degiovanni A. Détermination des diffusivités thermiques des matériaux anisotropes par méthode flash bidirectionnelle. J Phys III 1991;1(12):2027–46.
[17] Krapez JC, Spagnolo L, Friess M, Maier HP, Neuer G. Measurement of in-plane diffusivity in non-homogeneous slabs by applying flash thermography. Int J Therm Sci 2004;43(10):967–77.
[18] Spagnolo L, Krapez JC, Friess M, Maier HP, Neuer G. Flash thermography with a periodic mask: profile evaluation of the principal diffusivities for the control of composite materials. In: Proceedings of SPIE conference, Thermosense XXV, Orlando (USA); April, 2003.
[19] Rémy B, Degiovanni A, Maillet D. Measurement of the in-plane thermal diffusivity of materials by infrared thermography. Int J Thermophys 2005;26(2):493–505.
[20] Philippi I, Batsale JC, Maillet D, Degiovanni A. Measurement of thermal diffusivities through processing of infrared images. Rev Sci Instrum 1995;66(1):182–91.
[21] Angstrom AJ. Annalen der Physik und Chemie 1861;114:33; (also in English translation). Phil. Magazine and d. of Science 1863;25:130.
[22] Rochais D, Houëdec H, Enguehard F, Jumel J, Lepoutre F. Microscale thermal characterization at temperatures up to 1000 °C by photoreflectance microscopy. Application to the characterization of carbon fibres. J Phys D: Appl Phys 2005;38:1498–503.
[23] Pradere C, Goyheneche JM, Batsale JC, Dilhaire S, Pailler R. Thermal diffusivity measurements on a single fiber with microscale diameter at very high temperature. Int J Therm Sci 2006;45(5):443–51.
[24] Charles JA, Wilson DW. A model of passive thermal nondestrictive evaluation of composite laminates. Polym Compos 1981;2:105.
[25] Lecointe D. Caractérisation et simulation des processus de transferts lors d'injection de résine pour le procédé RTM. Ph.D. Thesis, Nantes University, 1999.
[26] Rolfes R, Hammerschmidt U. Transverse thermal conductivity of CFRP laminates: a numerical and experimental validation of approximation formulae. Comp Sci Technol 1995;54(1):45–54.
[27] Pal R. On the Lewis–Nielsen model for thermal/electrical conductivity of composites. Comp Part A 2008;39(5):718–26.
[28] Ning QG, Chou TW. Closed form solutions of the in-plane effective thermal conductivities of woven-fabric composites. Comp Sci Technol 1995;55(1):41–8.
[29] Hasselman DPH, Donaldson KY, Thomas JR. Effective thermal conductivity of uniaxial composite with cylindrically orthotropic carbon fibers and interfacial barrier. J Compos Mater 1993;27(6):637–44.
[30] Dasgupta A, Agarwal RK, Bhandarkar SM. Three-dimensional modeling of woven-fabric composites for effective thermo-mechanical and thermal properties. Compos Sci Technol 1996;56(3):209–23.
[31] Tavman IH. Effective thermal conductivity of isotropic polymer composites. Int Commun Heat Mass Trans 1998;25(5):723–32.
[32] Maxwell JC. A Treatise on Electricity and Magnetism. 3rd ed. New York: Dover; 1954 [chapter 9]. p. 1.
[33] Ning QG, Chou TW. A general analytical model for predicting the transverse effective thermal conductivities of woven fabric composites. Compos Part A 1998;29(3):315–22.
[34] Cox BN, Flanagan G. Handbook of analytical methods for textile composites. National Aeronautics and Space Administration; 1997.
[35] Informations on <http://www.toraycfa.com>.
[36] Sottos NR, Ockers JM, Swindeman M. Thermoelastic properties of plain weave composites for multilayer circuit board applications. J Electron Packag 1999;121(1):37–44.
[37] Rolfes R. Wärmeleitzahlen von UD-Laminaten aus CFK, Berechnung und Messung. Airbus & Institut für Strukturmechanik der DLR, 1991.
[38] Bailleul JL, Delaunay D, Jarny Y, Jurkowski T. Thermal conductivity of unidirectional reinforced composite materials: experimental measurement as a function of state of cure. J Reinf Plast Comp 2001;20(1):52–64.
[39] Sottos MSNR, Ockers JM. Thermoelastic properties of plain weave composites for multilayer circuit board applications. J Electron Packag 1999;121:37–43.
[40] Yamane T, Katayama S, Todoki M, Hatta I. The measurements of thermal conductivity of carbon fibers. J Wide Bandgap Mater 2000;7(4).